Title: **Post-translational mechanisms are associated with fertility restoration of cytoplasmic male sterility in sugar beet**

Authors: Kazuyoshi Kitazaki[1], Takumi Arakawa, Muneyuki Matsunaga, Rika Yui-Kurino, Hiroaki Matsuhira[2], Tetsuo Mikami and Tomohiko Kubo

Affiliations:
Research Faculty of Agriculture, Hokkaido University, N-9, W-9, Kita-ku, Sapporo, Hokkaido, 060-8589, Japan

Corresponding author: Tomohiko Kubo, Research Faculty of Agriculture, Hokkaido University, N-9, W-9, Kita-ku, Sapporo, 060-8589, Japan
tel/fax, +81-11-706-2484; e-mail, tomohiko@abs.agr.hokudai.ac.jp

Short title: Post-translational mechanisms in sugar beet CMS

Key words: cytoplasmic male sterility, fertility restoration, plant mitochondria, protein-protein interaction, *Beta vulgaris* ssp. *vulgaris*, Blue Native polyacrylamide gel electrophoresis

Word count: total, 7191; summary, 247; significant statement, 57; introduction, 813; results, 1923; discussion, 867; experimental procedures, 1317; acknowledgements, 74; short legends for supporting information, 90; references, 1073; figure legends, 717.

Present addresses:
[1]Horticulture Research Division, Kyushu Okinawa Agricultural Research Center, National Agriculture and Food Research Organization (NARO), Kurume, Fukuoka, 839-8503, Japan
[2]Crop Breeding Research Division, Hokkaido Agricultural Research Center, NARO, Sapporo, Hokkaido, 062-8555, Japan

SUMMARY

Genetic conflict between cytoplasmically inherited elements and nuclear genes due to their different transmission patterns can be seen in cytoplasmic male sterility (CMS), the mitochondrion-encoded inability to shed functional pollen. CMS is associated with a mitochondrial ORF absent from non sterility-inducing mitochondria (*S-orf*). Nuclear genes that suppress CMS are called *restorer-of-fertility* (*Rf*) genes. Post-transcriptional and translational repression of *S-orf* mediates the molecular action of *Rf* that encodes a class of RNA-binding proteins having pentatricopeptide repeat (PPR) motifs. Besides the PPR-type of *Rf*s, there are also non-PPR *Rf*s, but the molecular interactions between non-PPR *Rf* and *S-orf* have not been described. In this study, we investigated the interaction of sugar beet *bvORF20*, a non-PPR *Rf*, with *preSatp6*, the sugar beet *S-orf*. Anthers expressing bvORF20 contained a protein that interacted with preSATP6 protein. Analysis of anthers and transgenic calli expressing a FLAG-tagged *bvORF20* suggested binding of preSATP6 to bvORF20. To see the effect of bvORF20 on preSATP6, which exists as a 250-kDa protein-complex in CMS plants, signal bands of preSATP6 in *bvORF20*-expressing and non-expressing anthers were compared by immunoblotting combined with Blue Native polyacrylamide gel electrophoresis. The signal intensity of the 250-kDa band decreased significantly and 200- and 150-kDa bands appeared in *bvORF20*-expressing anthers. Transgenic callus expressing *bvORF20* also generated the 200- and 150-kDa bands. The 200-kDa complex likely includes both preSATP6 and bvORF20. Post-translational interaction between preSATP6 and bvORF20 appears to alter the higher order structure of preSATP6 that may lead to fertility restoration in sugar beet.

Significance Statement

Cytoplasmic male sterility (CMS) is expressed by the interaction of ORFs that are absent from non-male sterility-inducing mitochondria (*S-orf*) and nuclear genes called *restorer-of-fertility* (*Rf*) that suppress the CMS. In sugar beet, *S-orf* and *Rf* interact post-translationally, whereby a certain form of protein-complex consisting of *S-orf* translation products disappears in anthers where *Rf* is expressed.

INTRODUCTION

Heritable cytoplasmic elements are usually transmitted through only the female parent, whereas nuclear genes are transmitted through both the male and female parents. This difference in transmission pattern is thought to cause a genetic conflict in which certain cytoplasmic elements evolve to feminize the host organism to enhance their transmission, and the nuclear genome evolves suppressors against these selfish cytoplasmic elements (Werren, 2011). Evolution of cytoplasmic elements that feminize the hosts and nuclear genes that suppress the feminization are evident in cytoplasmic male sterility (CMS), a mitochondrially encoded trait that has been observed in more than 140 plant species (Laser and Lersten, 1972).

CMS has been associated with sterilizing mitochondria that express (often hydrophobic) proteins absent from nonsterilizing mitochondria (Hanson and Bentolila, 2004). Such proteins are encoded by ORFs unique to sterilizing mitochondrial genomes (Budar and Berthomé, 2007). The origin of these ORFs (hereafter termed *S-orf*s) is inferred to be recombination between (sometimes multiple) mitochondrial genes and/or unknown sequences, since *S-orf*s consist of parts of mitochondrial genes and/or origin-unknown sequences (Chase, 2007). Various *S-orfs* differing in their primary sequences have been reported (Budar and Berthomé, 2007). Some of these *S-orf*s probably impair mitochondrial respiratory chain complexes in a post-translational manner (Sabar *et al.*, 2003; Luo *et al.*, 2013). Other *S-orf*s are translated and form oligomers that are believed to exert deleterious effects on mitochondria (e.g. Duroc *et al.*, 2009). However, the significance of such oligomers on CMS expression is still unknown.

Accumulation of an *S-orf* translation product (S-ORF) is often low when the plant has a nuclear *restorer-of-fertility* gene (*Rf*), a suppressor of male sterility (Hanson and Bentolila, 2004) that probably evolved in the presence of *S-orf* (Touzet, 2012). Some of the *Rf*s that decrease S-ORF accumulation encode a class of protein having arrays of a degenerate motif termed a pentatricopeptide repeat (PPR) (Chen and Liu, 2014). Because PPR proteins are capable of binding RNA in sequence-specific manner (Barkan and Small, 2014), PPR-type *Rf*s are thought to be associated with post-transcriptional or translational repression of *S-orf* via direct interaction with *S-orf* mRNA (e.g. Kazama *et al.*

92 [2008] and Uyttewaal *et al.* [2008]), although indirect interaction has also been reported
93 (Hu *et al.*, 2012).
94 Post-transcriptional and translational mechanisms are not the only molecular means
95 for *Rf* suppression of *S-orf* action. For example, maize *Rf2* is a non-PPR type *Rf* encoding
96 a mitochondrial aldehyde dehydrogenase (Cui *et al.*, 1996). When a maize plant with
97 Texas-type CMS (CMS-T) has *Rf2*, accumulation of its S-ORF protein was unchanged
98 (Dewey *et al.*, 1987). On the other hand, the molecular mechanism that links maize RF2
99 and S-ORF is unknown. This holds true for the other non-PPR-type *Rf*s because their
100 molecular action on their cognate *S-orf*s is unknown.
101 Here, we show that a post-translational mechanism links a non-PPR-type *Rf* and *S-orf*
102 in sugar beet. The *S-orf* in sugar beet is likely *preSatp6*, an N-terminal extension (387
103 amino acid residues) of genuine *atp6*, a subunit of ATP synthase (Yamamoto *et al.*, 2005).
104 The nucleotide sequence of *preSatp6* has no significant homology to other *S-orf*s
105 (Yamamoto *et al.*, 2005). The translation product of *preSatp6* (preSATP6) is a membrane
106 protein that forms homo-oligomers (Yamamoto *et al.*, 2005). When sugar beet plants with
107 *Rf* were analyzed, transcription of *preSatp6* or accumulation of preSATP6 proteins was
108 unchanged (Yamamoto *et al.*, 2005). Therefore, whether post-transcriptional or
109 translational regulation was involved in the suppression of sugar beet CMS could not be
110 determined.
111 The nucleotide sequence of the locus containing one of the sugar beet *Rf*s, *Rf1*,
112 revealed a quadruplicated gene cluster, whose constituents are named *bvORF18* through
113 *bvORF21* (Matsuhira *et al.*, 2012). Only one of the constituents, *bvORF20*, was capable
114 of restoring partial pollen fertility to CMS sugar beet when expressed as a transgene
115 (Matsuhira *et al.*, 2012). *bvORF20* encodes a mitochondrial protein that resembles the
116 OMA1 metallopeptidase present in yeast and other eukaryotes (Käser *et al.*, 2003). Yeast
117 OMA1 was first identified as a protease involved in the protein quality-control system in
118 mitochondrial membranes, a process for coping with aberrant proteins (Leidhold and
119 Voos, 2007). Thus, it is possible that the *bvORF20*-translation product (bvORF20)
120 interacts with preSATP6. Although the peptidase activity of yeast and mammalian OMA1
121 is evident (Käser *et al.*, 2003; McBride and Soubannier, 2010), no peptidase activity is

expected from bvORF20 because its Zn^{2+}-binding site in the predicted proteolytic center has a glutamate-to-glutamine substitution that abolishes peptidase activity (Käser *et al.*, 2003; Matsuhira *et al.*, 2012). Thus, even if bvORF20 and preSATP6 interact with each other, degradation of preSATP6 appears to be unlikely.

In the present study, we first show protein-protein interaction between preSATP6 and bvORF20. We next show that the accumulation of a protein complex containing preSATP6 (probably the oligomeric form of preSATP6) is lower in fertility-restored anthers without a significant reduction in preSATP6 accumulation. Our data support the notion that certain conformations of S-ORF protein have functional significance in CMS expression.

RESULTS

The translation product of *bvORF20* is a membrane protein

An antiserum against bvORF20 (αbvORF20) was raised for protein analyses. The antigen corresponds to an internal region of bvORF20 and was expressed in *E. coli* as a recombinant protein. Note that the amino-acid sequences of bvORF18 through bvORF21 are so similar (88 to 100% identity) (Matsuhira *et al.*, 2012) that raising an antiserum that specifically reacts with bvORF20 is infeasible. Thus, αbvORF20 could react with bvORF18 through bvORF21 (OMA1-like proteins).

Total cellular proteins from anthers (collected before anthesis), taproots, and leaves of sugar beet line NK-198, from which *bvORF20* was cloned, were subjected to immunoblot analysis. We observed 41-kDa signal bands from immature anthers (Fig. 1a). The signal intensity was stronger in smaller anthers than larger ones. A very faint signal band was seen from the taproots but was barely visible in leaves. In a previous study, abundant transcripts of *bvORF18-bvORF21* were detected in flower buds by RNA gel blot analysis (Matsuhira *et al.*, 2012). Accumulation of *bvORF20* mRNA in immature anthers was confirmed by cDNA sequencing (Matsuhira *et al.*, 2012). We detected transcripts of *bvORF18-bvORF21* from roots by reverse transcription (RT) PCR analysis (Fig. S1), suggesting a low level of transcription of these genes in roots. Alternatively, a cross-reactable protein may exist in taproots. Altogether, the results of the immunoblot

152 analysis are consistent with the transcript analyses.

153 We expected membrane localization of the OMA1-like proteins, as is the case for
154 yeast OMA1 (Käser *et al.*, 2003). The soluble fraction of total cellular proteins from
155 immature anthers was subjected to immunoblot analysis using αbvORF20. Antisera
156 against preSATP6 (αpreSATP6) and MnSOD (αMnSOD) (Yamamoto *et al.*, 2005;
157 Bowler *et al.*, 1991), whose antigens are membrane and soluble proteins, respectively,
158 were used as controls. We used two sugar beet lines, NK-198 and TK-81mm-CMS, the
159 latter of which is a CMS line (i.e. having sterilizing mitochondria and being devoid of *Rf*).

160 As shown in Fig. 1b, αMnSOD reacted with both soluble and total proteins, and
161 αpreSATP6 reacted with total proteins but not with soluble proteins, indicating the
162 integrity of our sample preparation. The signal intensity of αpreSATP6 was
163 indistinguishable between NK-198 and TK-81mm-CMS, a result consistent with the
164 result of Yamamoto *et al.* (2005) who showed that accumulation of preSATP6 was
165 unchanged in the presence of *Rf*. The αbvORF20 reacted with a total lysate from NK-198
166 but not with the other samples (Fig. 1b). In a previous study by Matsuhira *et al.* (2012), a
167 chimeric green fluorescent protein having 55 N-terminal amino acid residues of
168 bvORF20 was localized to mitochondria. Taken together, these results indicate that
169 bvORF20 is a mitochondrial membrane protein.

170

171 **Protein-protein interaction between preSATP6 and bvORF20**

172 Because both preSATP6 and bvORF20 are membrane proteins, we expected that their
173 protein-protein interaction could be detected by immunoprecipitation (IP) analysis.
174 Immature anthers of NK-198 and TK-81mm-CMS were subjected to IP analysis using
175 αpreSATP6. Because preSATP6 is a highly hydrophobic protein, IP analysis was done in
176 the presence of a non-ionic detergent, digitonin (Eubel *et al.*, 2003). The precipitates were
177 resolved by SDS-polyacrylamide gel electrophoresis (PAGE) and visualized by gel
178 staining. As shown in Fig. 2a, 52-, 39-, and 28-kDa signal bands appeared when
179 TK-81mm-CMS was used. These bands correspond to the heavy chain of antibody (52
180 kDa), preSATP6 (39 kDa), and the light chain of antibody (28 kDa), respectively. On the
181 other hand, an additional 41-kDa signal band appeared in the lane for NK-198 (Fig. 2a).

We next examined whether the 41-kDa protein is an OMA1-like protein. Immunoprecipitates obtained using αpreSATP6 were subjected to immunoblot analysis. From the precipitate of NK-198 immature anthers, αbvORF20 reacted with a 41-kDa protein that was missing from the precipitate of TK-81mm-CMS (Fig. 2b), Anti-preSATP6 antiserum detected a 39-kDa signal band from NK-198 and TK-81mm-CMS, indicating that the sample was appropriately prepared (Fig. 2b). On the other hand, the reciprocal analysis in which immunoblots of αbvORF20 precipitates were probed with αpreSATP6 failed to detect any signal band (Fig. 2b). Considering the absence of αbvORF20 signal from αbvORF20 precipitates, a likely explanation is that there was insufficient exposure of the αbvORF20 epitope in the digitonin-lysed protein sample. In addition, difficulty in obtaining a sufficient amount of sugar beet anthers was an obstacle for further analysis of protein-protein interactions.

In order to confirm protein-protein interactions between preSATP6 and bvORF20, we generated transgenic callus that constitutively expressed *bvORF20* tagged with FLAG at the 3'-terminus (*bvORF20::flag*). Expression of the transgene was driven by the cauliflower mosaic virus (CaMV) 35S promoter. Sugar beet line NK-219mm-CMS, a CMS line, was used in these analyses because it is the only sugar beet line available to us that can be used for transgenic analyses (Kagami *et al.*, 2015).

The *bvORF20::flag* transgenic callus expressed the transgene as judged by the detection of 42-kDa signal band with anti-FLAG antiserum (αFLAG) (Fig S2). Considering the molecular mass of FLAG (~1 kDa), the size of the detected band is consistent with that of a fusion protein. Total cellular proteins from transgenic calli were lysed in digitonin. We prepared immunoprecipitates from this lysate using αFLAG, and the precipitates were electrophoresed and blotted. The blot was then probed with αpreSATP6. As shown in Fig. 3, a 39-kDa signal band appeared on the blot.

Our analysis included another transgene made from *bvORF20L*, the *bvORF20* counterpart of *rf1rf1* sugar beet lines (Matsuhira *et al.*, 2012; Moritani *et al.*, 2013). Although levels of transcripts and the translation products of *bvORF20L* were below the limits of detection by RNA gel blot analysis or immunoblot analysis (Matsuhira *et al.* [2012] and this study), transcription of *bvORF20L* was indicated by RT-PCR analysis

(Fig. S1). *bvORF20L* encodes a protein of 434 amino acid residues that are 83% identical to *bvORF20* (Matsuhira *et al.*, 2012). The protein products of the *bvORF20L::flag* transgene were detected in callus as shown in Fig. S2. We prepared αFLAG precipitates from the *bvORF20L::flag* callus; however, αpreSATP6 did not produce a 39-kDa signal band (Fig. 3). Therefore, although bvORF20 can bind to preSATP6, such an ability is likely absent from bvORF20L.

Decreased accumulation of the 250-kDa complex in fertility-restored anthers

Although bvORF20 resembles *Oma1*, the activity of bvORF20 on preSATP6 is not protein degradation as seen in Fig. 1. We tested another possibility that the consequence of bvORF20-preSATP6 interaction is a conformational alteration of preSATP6. In the previous study, preSATP6 was detected as a homo-oligomer on Blue Native (BN) polyacrylamide gels of proteins prepared with the detergent n-dodecyl D-maltoside (DDM) (Yamamoto *et al.*, 2005). Although digitonin, instead of DDM, was used in this study, preSATP6 was detected as a stable complex in the presence of digitonin (Fig. S3). No other polypeptides co-immunoprecipitated with preSATP6 in TK-81mm-CMS (Fig. 2). Therefore, the 250-kDa complex that was detected in the presence of digitonin may be a homo-oligomer.

We examined the oligomer status of preSATP6 in the immature anthers of NK-198. As shown in Fig. 4, a 200-kDa signal band appeared that is missing in TK-81mm-CMS. We also observed another signal band (150-kDa) in the NK-198 lane, but its signal intensity was fairly faint compared to that of the 200-kDa band. Furthermore, the signal intensity of the 250-kDa band in NK-198 was slightly reduced. The mobility of COXI-containing complexes was unchanged among TK-81mm-O, TK-81mm-CMS and NK-198 (Fig. 4). The electrophoretic mobility of a complex can be changed under different detergent/protein ratios (Eubel *et al.*, 2003); therefore, we tested whether the mobility of the 250-kDa complex was sensitive to the concentration of digitonin. Under our experimental conditions, the 250-kDa complex was stable (Fig. S4).

It is possible that the appearance of the 200- and 150-kDa complexes in NK-198 anthers was associated with bvORF20. If so, a correlation between expression of

242 *bvORF20* and the appearance of these two complexes would be expected. As seen in Fig.
243 1a, the expression of *bvORF20* decreased in accordance with anther development. If the
244 temporal expression pattern of *bvORF20* in anthers is more carefully measured, a
245 correlation between the expression of *bvORF20* and the appearance of these two
246 complexes can be tested using NK-198 anthers by sorting anthers by their developmental
247 stages.

248 Using a light microscope, we could distinguish seven developmental stages in
249 NK-198 anthers (Fig. S5) and confirmed that all five stamens in a flower developed
250 synchronously. As such, anther samples of each developmental stage were obtained by
251 the following procedure: for each flower, we determined the developmental stage of one
252 of the five anthers in the flower by light microscopy and the remaining four anthers were
253 sorted to the pool for the respective stage. Total cellular proteins of these pooled samples
254 were separated by SDS-PAGE. Immunoblot analysis using αbvORF20 revealed signal
255 bands from the meiosis, tetrad, and microspore stages, but the signal band was quite faint
256 from the mature stage (Fig. 5), indicating that *bvORF20* expression was very low in
257 anthers with mature pollen.

258 Next, protein samples of anthers at meiosis, tetrad (super pool of Ta, Tb and Tc of Fig.
259 5), microspore (super pool of Sa and Sb), and mature stages were lysed in digitonin and
260 electrophoresed in BN-polyacrylamide gels. Immunoblot analysis using αpreSATP6
261 revealed 200-kDa and (less intense) 150-kDa signal bands from meiosis, tetrad and
262 microspore anthers (Fig. 6). Such bands were faint in the mature anther sample. In this
263 blot, the signal intensity of the 250-kDa signal band was very low in the lanes containing
264 the 200- and 150-kDa bands. On the same blot, two complexes were detected with
265 αCOXI. The higher molecular mass complex consistently appeared in all the samples.
266 The lower molecular mass complex was missing from some lanes but this absence was
267 not correlated with the 200- and 150-kDa bands. Hence, the samples were appropriately
268 prepared. Therefore, *bvORF20* expression is probably associated with the appearance of
269 200- and 150-kDa complexes in NK-198 anthers. Whereas the signal patterns detected
270 with αpreSATP6 on BN-polyacrylamide gels differed among lanes of NK-198 proteins
271 (Fig. 6), the accumulation of preSATP6 was nearly constant during NK-198 anther

development, with a slight decrease at the early microspore stage (Fig. 5).

We expected that transgenic callus expressing *bvORF20* would have the 200- and 150-kDa complexes and that bvORF20 could be detected from at least one of these complexes. To test this hypothesis, total mitochondrial proteins from the *bvORF20::flag* transgenic callus were lysed in digitonin and subjected to two dimensional (2D) electrophoresis consisting of BN-PAGE for the first dimension and SDS-PAGE for the second dimension. Immunoblot analysis was carried out using αpreSATP6 and αFLAG. The antiserum αpreSATP6 cross-reacted with three spots (colored orange in Fig. 7a): spots corresponding to 250 kDa for the first dimension and 39 kDa for the second dimension (hereafter abbreviated as 250/39 kDa), 200/39 kDa, and 150/39 kDa. The mitochondrial protein from *bvORF20L::flag* transgenic callus, in which no interaction between preSATP6 and bvORF20L was detected (Fig. 3), had a 250/39-kDa spot but did not have 200/39-kDa or 150/39-kDa spots (Fig. 7b).

When the *bvORF20::flag* mitochondrial proteins on the blot were probed with αFLAG, we detected two spots, 200/42 kDa and 90/42 kDa (colored blue in Fig. 7a). The mobility of the 200/42-kDa spot in the first dimension appeared to be the same as that of the 200/39-kDa spot that was detected with αpreSATP6 (Fig. 7a), suggesting that bvORF20 and preSATP6 are components of the same 200-kDa complex. The 90/42-kDa signal spot suggested that bvORF20 forms another complex whose second constituent is unknown. The mitochondrial protein from *bvORF20L::flag* callus had only a 90/42-kDa signal spot when αFLAG was used (Fig. 7b). Therefore, bvORF20 is associated with the appearance of the 200- and 150-kDa complexes. Such ability is missing from bvORF20L.

DISCUSSION

We detected a protein-protein interaction between preSATP6 and bvORF20; the former is encoded by an *S-orf* and a gene in the sugar beet *Rf1* locus encodes the latter. Because bvORF20L, a recessive allele (i.e. incapable of CMS suppression), does not bind with preSATP6 nor affect the 250-kDa preSATP6 oligomer, the preSATP6-bvORF20 interaction may be associated with fertility restoration of sugar beet CMS.

Compared to other plant CMS systems involving PPR-type *Rfs*, the sugar beet system

is unique in terms of two points: (i) protein-protein interaction between bvORF20 and preSATP6, whereas PPR-type *Rf* gene products are thought to bind to mitochondrial mRNA (Chen and Liu, 2014); and (ii) preSATP6 accumulation is nearly unchanged in fertility-restored anthers even in the presence of bvORF20, whereas accumulation of S-ORF is reduced in fertility restored plants with PPR-type *Rf* (Hanson and Bentolila, 2004). These two distinguishing features could be expected given that *bvORF20* resembles *Oma1*, a member of the peptidase M48 family genes that has no RNA-binding activity as far as we know. In addition, whereas yeast and mammalian OMA1 can act as peptidases, no peptidase activity is expected from bvORF20 because of a crucial amino acid substitution in its Zn^{2+}-binding motif (Käser *et al.*, 2003; Matsuhira *et al.*, 2012).

The unique features of sugar beet CMS and fertility restoration may be implicated in the gene organization of *preSatp6*, which is an N-terminal extension of genuine *atp6* (Yamamoto *et al.*, 2005). The N-terminal extension of *atp6* plays an important role in the assembly of ATP6 with the mitochondrial ATPase complex in yeast (Zeng *et al.*, 2007). As the N-terminus of mature ATP6 has a serine-proline-leucine sequence, precursors of yeast ATP6 are likely proteolytically cleaved before the first serine (Michon *et al.*, 1988). N-terminal extension is ubiquitous in plant *atp6*, and the serine-proline-leucine motif is conserved in sugar beet and other plant *atp6* proteins (Krishnasamy *et al.*, 1994; Onodera *et al.*, 1999). Hence, plants may operate a post-translational system for ATP6 maturation similar to the yeast system. As for *preSatp6*, because no ATG codon is seen near the serine-proline-leucine motif, translation of *preSatp6* appears to be a prerequisite for expressing the downstream *atp6*. If translation of *preSatp6* were repressed by a post-transcriptional or translational mechanism, translation of the *atp6* would be simultaneously repressed.

Lack of an apparent decrease in preSATP6 accumulation in the fertility-restored plants is puzzling. In NK-198 plants, preSATP6 is detected from three different complexes, 250 kDa, 200 kDa and 150 kDa. The first complex is largely found in *bvORF20*-non-expressing tissues, and the latter two are from *bvORF20*-expressing tissues. The 250-kDa complex may be a homo-oligomer of preSATP6. Oligomer formation of S-ORF is often seen in other plant CMS systems, such as in radish (Duroc *et*

al., 2009). The functional significance of such an oligomer in disease susceptibility, and perhaps in male sterility, was proposed in maize CMS-T (Rhoads *et al.*, 1998). In NK-198, the 250-kDa complexes nearly disappear in meiotic and tetrad anthers. This temporal pattern is interesting if one considers that the first morphological abnormality of CMS anthers in sugar beet appears at the meiosis- or tetrad stages (Halldén *et al.*, 1991; Majewska-Sawka *et al.*, 1993). Perhaps the 250-kDa complex is harmful for anthers in these developmental stages; hence, reduction of the 250-kDa complex restores pollen fertility. This hypothesis may imply that preSATP6 protein *per se* is not directly responsible for CMS but its 250-kDa complex form is; however, further study is necessary to examine this possibility.

Meiotic and tetrad anthers of NK-198 were characterized by the appearance of 200-kDa and 150-kDa complexes containing preSATP6. The two complexes simultaneously appeared in the anther where *bvORF20* was expressed. The appearance of these two complexes was reproduced in transgenic calli expressing *bvORF20*, and whose translation products bound preSATP6. Collectively, these results suggest that *bvORF20* plays a principal role in this phenomenon. Possibly bvORF20 traps nascent preSATP6 before it assembles into a 250-kDa complex and/or bvORF20 intrudes into the 250 kDa complex to dissociate the complex. In calli expressing *bvORF20*, the 250-kDa complex remained visible on the blot in spite of the strong expression of *bvORF20::flag*. Therefore, the efficiency of *bvORF20* on the 250-kDa complex may be influenced by physiological condition (i.e. callus vs. anther). For example, the rate of *preSatp6* expression may be affected by a physiological condition, and/or an additional supporting factor that is absent from calli may exist in meiotic and tetrad-stage anthers.

The precise relationship between the 200-kDa and the 150-kDa complexes is unknown. One possibility is that initially bvORF20 binds to preSATP6 (at an unknown molar ratio) to form the 200-kDa complex, then the 150-kDa complex is formed by releasing bvORF20. It is also possible that the 150-kDa complex, and/or the 200-kDa complex, is further converted into indiscriminate-sized complexes, a possible explanation for the rather smeared image in the lanes of NK-198 anthers (Figs. 4 and 6). Although the molecular chaperone-like activity of bvORF20 is necessary for this scenario, it can be

362 invoked by comparison with that of yeast OMA1, which is suggested to have the ability to
363 dislocate its substrate proteins from membranes (Käser *et al.*, 2003). In support of this
364 hypothesis, functional and evolutionary relationships between bvORF20 and genuine
365 OMA1 should be examined.
366
367 **EXPERIMENTAL PROCEDURES**
368 **Plant materials**
369 All the sugar beet lines used in this study were developed at the Hokkaido Agricultural
370 Research Center, National Agriculture and Food Research Organization, Memuro, Japan.
371 NK-198 is a fertility-restored line that has CMS mitochondria but is fully male fertile due
372 to *Rf* (Matsuhira *et al.*, 2012). TK-81mm-CMS is a male sterile (MS) line having CMS
373 mitochondria but no *Rf* (Satoh *et al.*, 2004). TK-81mm-O has the same nuclear genotype
374 as TK-81mm-CMS but is male fertile due to nonsterilizing mitochondria (Satoh *et al.*,
375 2004). NK-219mm-CMS is another MS line with CMS mitochondria, but its genotype is
376 known to be suitable for generating transgenic sugar beet plants (Kagami *et al.*, 2015).
377
378 **Transgene construction**
379 The backbone of the binary vectors was pMDCΩ that was constructed as follows: a
380 region containing the 35S promoter of cauliflower mosaic virus (CaMV) and the omega
381 prime translation leader of tobacco mosaic virus was PCR amplified from pFGC5941
382 (Kerschen *et al.*, 2004) with primer 1 (see Table S1 for all oligo nucleotide primer
383 sequences) and primer 2. The resulting PCR products were digested with *Hin*dIII and
384 *Asc*I (Takara Bio, Ohtsu, Japan) to generate cohesive ends. Plasmid DNAs of pMDC32
385 (Curtis and Grossniklaus, 2003), a binary vector equipped with the Gateway system
386 (Invitrogen, Carlsbad, CA), were digested with *Hin*dIII and *Asc*I to remove the original 2
387 x CaMV35S promoter region and to generate cohesive ends. Plasmid DNA and the
388 restriction-digested PCR products were ligated to yield pMDCΩ.
389 The binary vector containing *bvORF20::flag* was constructed as follows: Matsuhira
390 *et al.* (2012) constructed a plasmid containing the genomic *bvORF20* region, from which
391 the open reading frame (ORF) of *bvORF20* including its 5'- and 3'-untranslated regions

(UTRs) was amplified with primers 3 and 4. The resulting PCR fragment was inserted into pDONRzeo, a donor vector for the Gateway system (Invitrogen), using the BP Clonase Enzyme mix (Invitrogen) according to the manufacturer's instructions. Plasmid DNA was subjected to PCR amplification with primers 5 and 6, two overlapping primers that correspond to the junction between *bvORF20* ORF and its 3'-UTR; thirty-two base pairs of the two primers are complementary to each other, and the two primers are designed to fuse the *flag* tag to the 3'-end of *bvORF20*. The PCR products (i.e. linear plasmid DNA with 32-bp complementary ends) were digested with *Dpn*I, a restriction enzyme that requires methylated adenine at its recognition site for cleavage, to destroy residual plasmid DNA. The constructs were then introduced into *E. coli* by electroporation. Circular plasmid DNA is restored in transformed *E. coli* via DNA recombination (*Dpn*I mediated site-directed mutagenesis). After confirming the nucleotide sequence of the recovered plasmid DNA from a colony selected from a selective plate, the insert DNA was transferred to pMDCΩ using the LR Clonase Enzyme mix (Invitrogen).

The binary vector containing *bvORF20L::flag* was constructed as follows: the *bvORF20L* ORF as well as its 5'- and 3'-UTRs was PCR amplified with primers 7 and 8 from genomic DNA of TK-81mm-O. PCR products were cloned into pDONRzero using BP Clonase Enzyme mix. After confirming the nucleotide sequence, the plasmid DNA was subjected to PCR amplification with primers 5 and 6, and the PCR products were subjected to the *Dpn*I mediated site-directed mutagenesis to recover *bvORF20L::flag* plasmid DNA. After nucleotide sequence confirmation, the insert DNA was transferred to pMDCΩ by LR Clonase Enzyme mix.

Generation of transgenic callus

Procedures to obtain transgenic callus were as described in Kagami *et al*. (2015). Briefly, callus was induced from leaf explants that were harvested from *in vitro* germinated plantlets of NK-219mm-CMS. Suspension cells were established from the callus and infected with *Agrobacterium tumefaciens* strain LBA4404 containing the transgene. After infection, the suspension cells were placed on a selective medium that contained

hygromycin. Resistant colonies were transferred onto new selective medium. Transgenic calli were grown until they reached a fresh weight of ~200mg for protein preparation.

Preparation of antisera

For antigen preparation, a DNA fragment corresponding to E191 to E270 of bvORF20 was PCR amplified by primers 13 and 14 from *bvORF20* cDNA using LA Taq (Takara Bio, Ohtsu, Japan). The PCR fragment was subjected to the second PCR using primers 15 and 16 to add the attB site for Gateway cloning and cloned into donor vector pDONR201 (Invitrogen) using BP Clonase Enzyme Mix. After verifying the sequence integrity, the inserted DNA fragments were transferred to binary vector pDEST17 (Invitrogen) using LR Clonase Enzyme Mix, and the resulting plasmid was introduced into *E. coli* strain BL21 (SI). The fusion protein tagged with 6 x His was purified using Pro Bond Resin (Invitrogen) and separated by SDS-PAGE. The fusion protein was electrophoretically eluted from gel slices using an Electro Eluter Model 422 (Bio-Rad Laboratories, Hercules, CA). Immunization of rabbits and preparation of antisera were performed according to standard methods (Sambrook *et al.*, 1989). The antiserum was purified by HiTrap rProtein A FF Columns (GE Healthcare UK, Amersham Place, England) according to the manufacturer's instructions. αMnSOD and αFLAG were purchased from Sigma-Aldrich (St Louis, MO) and Medical and Biological Laboratories (Nagoya, Japan), respectively. Details about the preparation of αpreSATP6 and αCOXI were described previously (Yamamoto *et al*., 2005).

Protein preparation

Root mitochondria were isolated according to the methods of Lind *et al.* (1991) and stored at -80ºC until use. Crude mitochondria from transgenic calli were isolated as follows: callus (~200mg) was ground in an Eppendorf tube with a plastic pestle in the presence of isolation buffer [50mM Tris-HCl (pH8.0), 0.5M mannitol, 1mM Na_2·EDTA, 0.1% bovine serum albumin, 1.0% L-Na·ascorbate, and 0.5% polyclar AT] at 4˚C. The ground products were centrifuged twice (5500*g*, 10min, 4˚C and 6500*g*, 15min, 4˚C) to obtain the supernatant. The supernatant was centrifuged (11500*g*, 15min, 4˚C), and the

pellet was resuspended in wash buffer [50mM Tris-HCl (pH8.0), 0.5M mannitol, 1mM Na_2·EDTA]. This step was repeated once. The final pellet was resuspended in the wash buffer and used as crude mitochondria. Materials for total-cellular-protein extraction were flower buds, anthers, leaves and root tissues that were powdered in liquid nitrogen. For SDS-PAGE, mitochondria or powdered tissues were boiled in SDS extraction buffer [2%(w/v) SDS, 10%(v/v) glycerol, 1%(v/v) 2-mercaptoethanol, 0.001% (w/v) bromophenol blue, 50mM Tris-HCl (pH6.8)] for 5 min, centrifuged at 13000*g* for 5min, and the supernatants were used for experiments. The soluble fraction was extracted by mixing powdered tissue with a buffer containing 25mM Tris-HCl (pH 6.8) and 5% glycerol followed by centrifuging at 13000*g* for 5min. The supernatant was boiled for 5 min after the addition of 2x SDS-PAGE buffer [4%(w/v) SDS, 20%(v/v) glycerol, 2%(v/v) 2-mercaptoethanol, 0.002% (w/v) bromophenol blue, 100mM Tris-HCl (pH6.8)]. For BN-PAGE and immunoprecipitation assays, powdered tissues were incubated on ice for 30 min in 1 x Native–PAGE sample buffer (Invitrogen) (or PBS) containing digitonin and Protein Inhibitor Cocktail for plant cell and tissue extracts (Sigma). Unless otherwise mentioned, the digitonin/sample protein ratio (w/w) was 5.0. After adding Benzonase Nuclease (Takara Bio or Merck Millipore, Billerica, MI) and $MgCl_2$ (2 mM final concentration), the samples were incubated at room temperature for 30 min, then centrifuged at 33000*g* for 30min, and the supernatants were used for experiments. When root mitochondrial protein was used for BN-PAGE, the Benzonase Nuclease treatment was omitted. Protein concentrations were determined by a modified Lowry method using a DC protein assay kit (Bio-Rad Laboratories) with BSA as the reference.

Immunoprecipitation assay

Dynabeads Protein G (Invitrogen) were used according to the manufacturer's instructions.

Electrophoresis and immunoblot analysis

SDS-PAGE was performed according to the method of Schägger and von Jagow (1987). BN–PAGE and 2D electrophoresis were performed using the Native PAGE Novex

BisTris Gel system (Invitrogen) according to the manufacturer's instructions. Gels were stained using Rapid CBB KANTO (Kanto Chemical, Tokyo, Japan) or Deep Purple Total Protein Stain (GE Healthcare) according to the manufacturer's instructions, respectively. Separated proteins were electroblotted onto Hybond-P (GE Healthcare) using a Mini TransBlot Cell (Bio-Rad Laboratories). Chemiluminescent signals were detected using ECL-Plus or ECL-Advance (GE Healthcare) according to the manufacturer's instructions.

CONFLICT OF INTEREST

The authors declare that they have no conflict of interest.

ACKNOWLEDGMENTS

We thank Dr. Kazunori Taguchi and Dr. Yosuke Kuroda for providing seeds and Dr. Francoise Budar for her invaluable comments. This work was supported in part by MEXT/JSPS KAKENHI Grant Number to 18075001, 22580001, and 25292001; Grants-in-Aid for Scientific Research from the Program for Promotion of Basic and Applied Researches for Innovations in Bio-oriented Industry (BRAIN); and Grants-in-Aid for Science and Technology Research Promotion Program for Agriculture, Forestry, Fisheries and Food Industry, Japan.

SUPPORTING INFORMATION

Figure S1. Reverse transcription PCR of *Oma1*-like genes encoded by the sugar beet *Rf1* locus.

Figure S2. Immunoblot analysis of sugar beet calli that were resistant to hygromycin.

Figure S3. Detection of a complex containing preSATP6.

Figure S4. Immunoblot analysis of immature anthers collected from TK-81mm-CMS.

Figure S5. Light microscopic images of anther contents stained with Alexander's dye.

Figure S6. Immunoblot analysis of mitochondrial proteins from NK-219mm-CMS callus expressing *bvORF20::flag*.

Figure S7. Immunoblot analysis of mitochondrial proteins from NK-219mm-CMS callus

512 expressing *bvORF20L::flag*.

513 **Table S1.** Nucleotide sequences of primers.

514

515 **REFERENCES**

516 Barkan, A. and Small, I. (2014) Pentatricopeptide repeat proteins in plants. *Annu. Rev.*
517 *Plant Biol.* 65, 415-442.

518 Bowler, C. Slooten, L., Vandenbranden, S., De Rycke, R., Botterman, J., Sybesma, C.,
519 Van Montagu, M. and Inzé, D. (1991) Manganese superoxide dismutase can reduce
520 cellular damage mediated by oxygen radicals in transgenic plants. *EMBO J.* 10,
521 1723-1732.

522 Budar, F and Berthomé, R. (2007) Cytoplasmic male sterilities and mitochondrial gene
523 mutations in land plants. In *Plant Mitochondria* (Logan, D.C., ed). Oxford:
524 Blackwell Publishing, pp 278–307.

525 Chase, C.D. (2007) Cytoplasmic male sterility: a window to the world of plant
526 mitochondrial-nuclear interactions. *Trends Genet.* 23, 81-90.

527 Chen, L. and Liu, Y.-G. (2014) Male sterility and fertility restoration in crops. *Annu. Rev.*
528 *Plant Biol.* 65, 579-606.

529 Cui, X., Wise, R.P. and Schnable, P.S. (1996) The *rf2* nuclear restorer gene of male-sterile
530 T-cytoplasm maize. *Science* 272, 1334-1336.

531 Curtis, M.D. and Grossniklaus, U. (2003) A gateway cloning vector set for
532 high-throughput function analysis of genes in planta. *Plant Physiol.* 133, 462-469.

533 Dewey, R.E., Timothy, D.H. and Levings, C.S. III (1987) A mitochondrial protein
534 associated with cytoplasmic male sterility in the T cytoplasm of maize. *Proc. Natl.*
535 *Acad. Sci. USA* 84, 5374-5378.

536 Duroc, Y., Hiard, S., Vrielynck, N., Ragu, S. and Budar, F. (2009) The Ogura
537 sterility-inducing protein forms a large complex without interfering with the
538 oxidative phosphorylation components in rapeseed mitochondria. *Plant Mol. Biol.* 70,
539 123-137.

540 Eubel, H., Jänsch, L. and Braun, H.P. (2003) New insights into the respiratory chain of
541 plant mitochondria. Supercomplexes and a unique composition of complex II. *Plant*

Physiol. 133, 274-286.

Halldén, C., Karlsson, G., Lind, C., Møller, I.M. and Heneen, W.K. (1991) Microsporogenesis and tapetal development in fertile and cytoplasmic male-sterile sugar beet (*Beta vulgaris* L.). *Sex. Plant Rep.* 4, 215-225.

Hanson, M.R. and Bentolila, S. (2004) Interactions of mitochondrial and nuclear genes that affect male gametophyte development. *Plant Cell* 16, S154-S169.

Hu, J. Wang, K., Huang, W. *et al.* (2012) The rice pentatricopeptide repeat protein RF5 restores fertility in Hong-Lian cytoplasmic male-sterile lines via a complex with the glycine-rich protein GRP162. *Plant Cell* 24, 109-122.

Kagami, H., Kurata, M., Matsuhira, H., Taguchi, K., Mikami, T., Tamagake, H. and Kubo, T. (2015) Sugar beet (*Beta vulgaris* L.). In *Agrobacterium Protocols (Methods in Molecular Biology 1223)* (Wang, K. ed). New York: Springer, pp. 335-347.

Käser, M., Kambacheld, M., Kisters-Woike, B. and Langer, T. (2003) Oma1, a novel membrane-bound metallopeptidase in mitochondria with activities overlapping with the *m*-AAA protease. *J. Biol. Chem.* 278, 46414-46423.

Kazama, T., Nakamura, T., Watanabe, M., Sugita, M. and Toriyama, K. (2008) Suppression mechanism of mitochondrial ORF79 accumulation by Rf1 protein in BT-type cytoplasmic male sterile rice. *Plant J.* 55, 619-628.

Kerschen, A., Napoli, C.A., Jorgensen, R.A. and Müller, A.E. (2004) Effectiveness of RNA interference in transgenic plants. *FEBS lett.* 566, 223-228.

Krishnasamy, S., Grant, R.A. and Makaroff, C.A. (1994) Subunit 6 of the F_0-ATP synthase complex from cytoplasmic male-sterile radish: RNA editing and NH_2-terminal protein sequencing. *Plant Mol. Biol.* 24, 129-141.

Laser, K.D. and Lersten, N.R. (1972) Anatomy and cytology of microsporogenesis in cytoplasmic male sterile angiosperms. *Bot. Rev.* 38, 425-454.

Leidhold, C. and Voos, W. (2007) Chaperones and proteases – guardians of protein integrity in eukaryotic organelles. *Ann. N. Y. Acad. Sci.* 1113, 72-86.

Lind, C., Halldén, C. and Møller, I.M. (1991) Protein synthesis in mitochondria purified from roots, leaves and flowers of sugar beet. *Physiol. Plant.* 83, 7-16.

Luo, D., Xu, H., Liu, Z. *et al.* (2013) A detrimental mitochondrial-nuclear interaction

causes cytoplasmic male sterility in rice. *Nat. Genet.* 45, 573-577.

Majewska-Sawka, A., Rodriguez-Garcia, M.I., Nakashima, H. and Jassen, B. (1993) Ultrastructural expression of cytoplasmic male sterility in sugar beet (*Beta vulgaris* L.). *Sex. Plant Rep.* 6, 22-32.

Matsuhira, H., Kagami, H., Kurata, M. *et al.* (2012) Unusual and typical features of a novel *restorer-of-fertility* gene of sugar beet (*Beta vulgaris* L.). *Genetics* 192, 1347–1358.

McBride, H. and Soubannier, V. (2010) Mitochondrial function: OMA1 and OPA1, the grandmasters of mitochondrial health. *Curr. Biol.* 20, R274-R276.

Michon, T., Galante, M. and Velours, J. (1988) NH_2-terminal sequence of the isolated yeast ATP synthase subunit 6 reveals post-translational cleavage. *Eur. J. Biochem.* 172, 621-625.

Moritani, M., Taguchi, K., Kitazaki, K., Matsuhira, H., Katsuyama, T., Mikami, T. and Kubo, T. (2013) Identification of the predominant nonrestoriong allele for Owen-type cytoplasmic male sterility in sugar beet (*Beta vulgaris* L.): development of molecular markers for the maintainer genotype. *Mol. Breed.* 32, 91-100.

Onodera, Y., Yamamoto, M.P. Kubo, T. and Mikami, T. (1999) Heterogeneity of the *atp6* presequences in normal and different sources of male-sterile cytoplasms of sugar beet. *J. Plant Physiol.* 155, 656-660.

Rhoads, D.M., Brunner-Neuenschwander, B., Levings, C.S. III and Siedow, J.N. (1998) Cross-linking and disulfide bond formation of introduced cysteine residues suggest a modified model for the tertiary structure of URF13 in the pore-forming oligomers. *Arch. Biochem. Biophys.* 354, 158-164.

Sabar, M., Gagliardi, D., Balk, J. and Leaver, C.J. (2003) ORFB is a subunit of F_1F_0-ATP synthase: insight into the basis of cytoplasmic male sterility in sunflower. *EMBO Rep.* 4, 381-386.

Sambrook, J., Fritsch, E.F. and Maniatis, T. (1989) *Molecular Cloning: A Laboratory Manual*. Cold Spring Harbor: Cold Spring Harbor Laboratory Press.

Satoh, M., Kubo, T., Nishizawa, S., Estiati, A., Itchoda, N. and Mikami, T. (2004) The cytoplasmic male-sterile type and normal type mitochondrial genomes of sugar beet

602 share the same complement of genes of known function but differ in the content of
603 expressed ORFs. *Mol. Gen. Genomics* 272, 247-256.
604 Schägger, H. and von Jagow, G. (1987) Tricine-sodium dodecyl sulfate-polyacrylamide
605 gel electrophoresis for the separation of proteins in the range from 1 to 100 kDa. *Anal.*
606 *Biochem.* 166, 368-379.
607 Touzet, P. (2012) Mitochondrial genome evolution and gynodioecy. In *Mitochondrial*
608 *Genome Evolution (Advances in Botanical Research volume 63)*. (Marechal-Drouard,
609 L., ed). Oxford: Academic Press, pp 71-98.
610 Uyttewaal, M. Arnal, N., Quadrado, M. *et al.* (2008) Characterization of *Raphanus*
611 *sativus* pentatricopeptide repeat proteins encoded by the fertility restorer locus for
612 Ogura cytoplasmic male sterility. *Plant Cell* 20, 3331-3345.
613 Werren, J.H. (2011) Selfish genetic elements, genetic conflict, and evolutionary
614 innovation. *Proc. Natl. Acad. Sci. USA* 108, 10863-10870.
615 Yamamoto, M.P., Kubo, T. and Mikami, T. (2005) The 5'-leader sequence of sugar beet
616 mitochondrial *atp6* encodes a novel polypeptide that is characteristic of Owen
617 cytoplasmic male sterility. *Mol. Genet. Genomics* 273, 342–349.
618 Zeng, X., Kuchatczyk, R., di Rago, J.P. and Tzagoloff, A. (2007) The leader peptide of
619 yeast Atp6p is required for efficient interaction with the Atp9p ring of the
620 mitochondrial ATPase. *J. Biol. Chem.* 282, 36167-36176.
621
622

623 Figure legends

624

625 **Fig. 1.** Immunoblot analysis of sugar beet organs. **a.** Total cellular proteins of immature
626 anthers (lanes 1 and 2), taproots (3) and leaves (4) from sugar beet line NK-198 were
627 electrophoresed in a 12% SDS polyacrylamide gel and probed with αbvORF20.
628 Immature anthers were sampled from anthers before anthesis. The proteins of lane 1 were
629 prepared from smaller and greenish anthers, and the proteins of lane 2 were from larger
630 and yellowish (i.e. further developed) anthers. The 41-kDa signal band is indicated by an
631 arrow. Size markers are shown on the left (in kDa). The same proteins as shown in lanes 1
632 to 4 were electrophoresed and stained with Coomassie brilliant blue (CBB). **b.** Total (T)
633 and soluble (S) fractions of total cellular proteins of immature anthers (both greenish and
634 yellowish ones) from TK-81mm-CMS (CMS) and NK-198 (Rf1) were electrophoresed in
635 a 12% SDS polyacrylamide gel and probed with αbvORF20, αpreSATP6, or αMnSOD.
636 The apparent molecular mass is shown on the right (kDa).

637

638 **Fig. 2.** Detection of protein-protein interactions between preSATP6 and bvORF20. **a.**
639 Immunoprecipitation analysis of immature anther proteins lysed in digitonin using
640 αpreSATP6 (12% SDS-PAGE). Signal bands were visualized by fluorescent staining.
641 Immature anthers were collected from TK-81mm-CMS (lane 1) and NK-198 (lane 2).
642 Signal band of a 41-kDa protein is indicated by an arrow. Size markers are shown on the
643 left. **b.** Immunoblot analysis against immunoprecipitates (IP) of immature anthers lysed
644 in digitonin. Immature anthers were collected from TK-81mm-CMS and NK-198.
645 Precipitates were obtained using αbvORF20 or αpreSATP6 as indicated on the top of the
646 images. The positive control was total lysate (Input). The negative control was prepared
647 using the same procedure as for the immunoprecipitates without antiserum (-). Antisera
648 used for signal band detection (IB) were αpreSATP6, αbvORF20, and αCOXI. Apparent
649 molecular masses are shown on the right (kDa).

650

651 **Fig. 3.** Detection of protein-protein interactions between preSATP6 and transgenic
652 bvORF20 tagged with FLAG. Anti-FLAG antiserum precipitated proteins (IP) were

prepared from callus expressing *bvORF20::flag* (20-FLAG), *bvORF20L::flag* (20L-FLAG), and callus of non-transgenic NK-219mm-CMS (NT). Total lysates were included in this experiment (Input). Protein gel bots were probed with αpreSATP6, αFLAG, or αCOXI. The apparent molecular mass is shown on the right (kDa).

Fig. 4. Immunoblot analysis of immature anthers collected from TK-81mm-O (lane 1), TK-81mm-CMS (2), and NK-198 (3). Total cellular proteins were lysed in digitonin and electrophoresed in a Blue Native-polyacrylamide gel (3-12%). Gel blots were probed with αpreSATP6 or αCOXI. Open and filled arrows indicate the 200 kDa and 150-kDa signal bands, respectively. Size markers are shown on the left (kDa).

Fig. 5. Immunoblot analysis of immature anthers collected from TK-81mm-O (indicated by label 1), TK-81mm-CMS (label 2), and NK-198 (label 3). Abbreviations of samples are: Ig, small, greenish immature anthers; Iy, large, yellowish immature anthers; M, meiosis stage; Ta, early tetrad stage; Tb, middle tetrad stage; Tc, late tetrad stage; Sa, early microspore stage; Sb, late microspore stage; P, mature stage. For details about anther developmental stages, see Fig. S5. Total cellular proteins were electrophoresed in SDS-polyacrylamide gels (12%), and probed with αbvORF20, αpreSATP6, or αCOXI. Apparent molecular masses of the signal bands are shown on the right (kDa).

Fig. 6. Immunoblot analysis of immature anthers collected from TK-81mm-O (indicated by label 1), TK-81mm-CMS (label 2), and NK-198 (label 3). Abbreviations of samples are: I, pooled immature anthers of various developmental stages; M, meiosis stage; T, super pool of Ta, Tb, and Tc identified in Fig. 5; S, super pool of Sa and Sb identified in Fig. 5; P, mature stage. Total cellular proteins were lysed in digitonin and electrophoresed in a Blue Native-polyacrylamide gel (3-12%). Gel blots were probed with αpreSATP6 or αCOXI. Size markers are shown on the left (kDa).

Fig. 7. Merged images of immunoblot analyses. Signal spots detected by αpreSATP6 and αFLAG are colored orange and blue, respectively. The samples were lysed in digitonin

683 and subjected to 2D electrophoresis consisting of BN-PAGE (3-12%) for the first
684 dimension (from left to right) and SDS-PAGE (4-12%) for the second dimension (from
685 top to bottom). Size markers are shown on the top and left (kDa). For the original images,
686 see Figs. S6 and S7. **a.** Total mitochondrial proteins isolated from NK-219mm-CMS
687 callus expressing the *bvORF20::flag* transgene. **b.** Total mitochondrial proteins isolated
688 from NK-219mm-CMS callus expressing the *bvORF20L::flag* transgene.
689

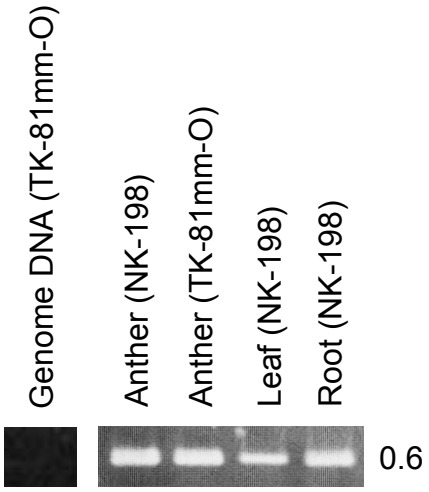

Fig. S1. Reverse transcription PCR of *Oma1*-like genes encoded by the sugar beet *Rf1* locus. NK-198 (fertility restored line) and TK-81mm-O (maintainer line which is devoid of any *Rf* but male fertile due to lack of *S-orf* from mitochondria) were used in this experiment. Anthers, leaves, and roots of NK-198, and anthers of TK-81mm-O were the tissues used in this analysis. Total cellular RNA was extracted with an RNeasy Plant Mini Kit (Qiagen, Valencia, CA), and treated with RNase-free DNase I (Takara Bio, Ohtsu, Japan). Complementary DNA was obtained using SuperScript III First-Strand Synthesis System (Invitrogen, Carlsbad, CA). Nucleotide sequences of primers are 5'-TTTGGAAGGGATGAATTGGG-3' and 5'-CATAACATCAGCTCGAGCTAA-3', which correspond to the first intron and the third intron, respectively. A size marker is shown on the right (kbp). The target sequences of these primers are conserved between NK-198 and TK-81mm-O copies. The PCR protocol was 30 cycles of 94˚C, 30 sec, 58˚C, 30 sec, and 72˚C, 2 min. PCR products were electrophoresed in a 2% agarose gel. Integrity of the TK-81mm-O amplicon was confirmed by nucleotide sequencing. No 0.6-kbp signal band was seen when genomic DNA of TK-81mm-O was used as the template.

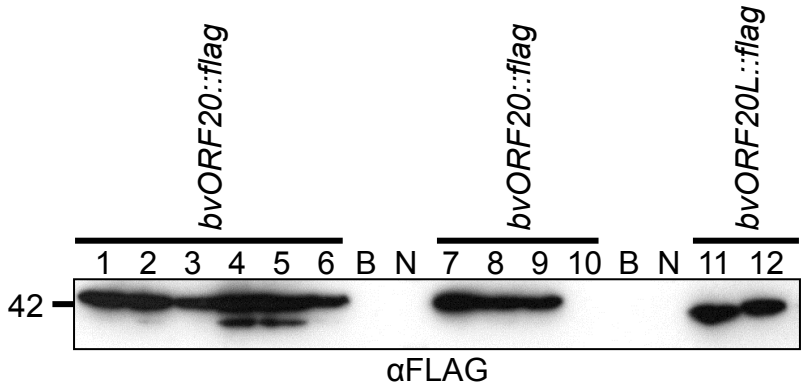

Fig. S2. Immunoblot analysis of sugar beet calli that were resistant to hygromycin. Sugar beet suspension cells were infected with *Agrobacterium* transformed with the *bvORF20::flag* transgene or the *bvORF20L::flag* transgene, then grown on a medium containing hygromycin. Total cellular proteins from ten (lanes 1-10) and two (11-12) calli, candidates having *bvORF20::flag* and *bvORF20L::flag*, respectively, were electrophoresed in a 12% SDS-polyacrylamide gel. The blot was probed with anti-FLAG antiserum (αFLAG). A size marker is shown on the left (kDa). B and N denote blank and non-transgenic callus, respectively.

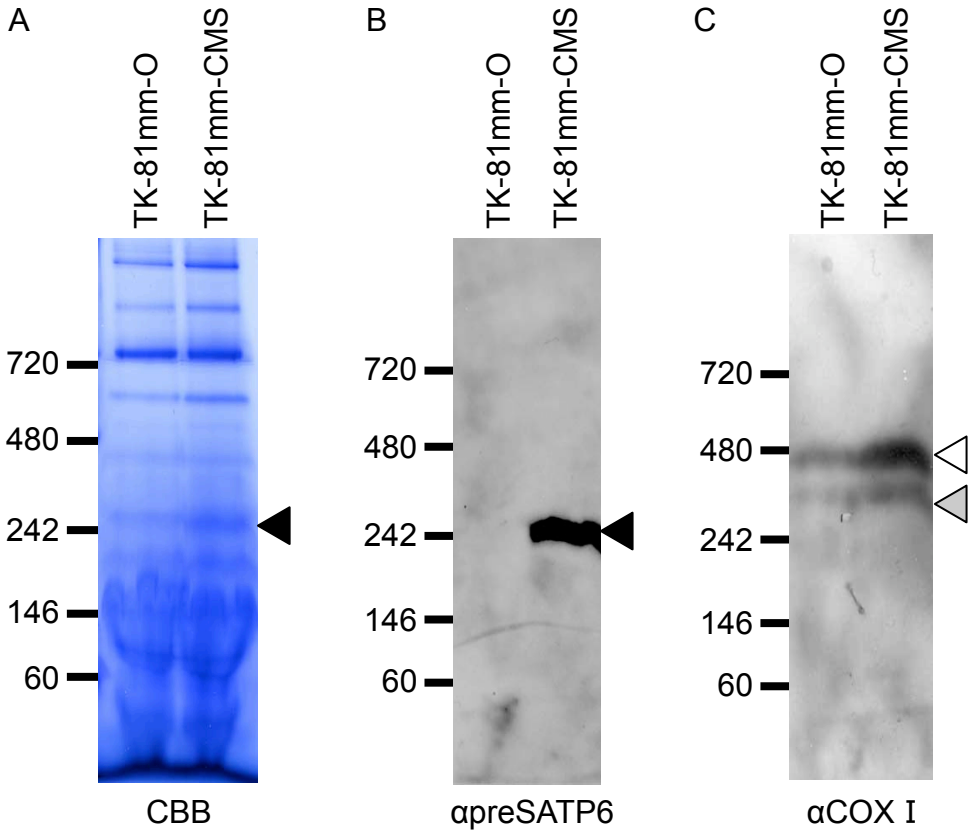

Fig. S3. Detection of a complex containing preSATP6. Size markers are shown to the left of each image (kDa). **A.** Blue Native (BN) polyacrylamide gel electrophoresis (PAGE) (3-12%) of mitochondrial proteins prepared from TK-81mm-O and TK-81mm-CMS taproots. Proteins were prepared in the presence of digitonin (the digitonin/ protein ratio was 5.0 [w/w]). The gel was stained with Coomassie brilliant blue (CBB). The obtained electrophoretic patterns were very similar between the two sugar beet lines except for the 250 kDa signal band that was specific to TK-81mm-CMS. A filled triangle indicates the 250 kDa signal band specific to TK-81mm-CMS. **B.** Gel blot analysis of proteins separated in panel A. Anti-preSATP6 (αpreSATP6) antiserum was used. A filled triangle indicates the 250 kDa signal band. **C.** Gel blot analysis of proteins separated in panel A. Anti COXI antiserum (αCOXI) was used. Open and shaded triangles indicate the 420 and 340 kDa signal bands (the two super complexes containing mitochondrial Complex IV), respectively.

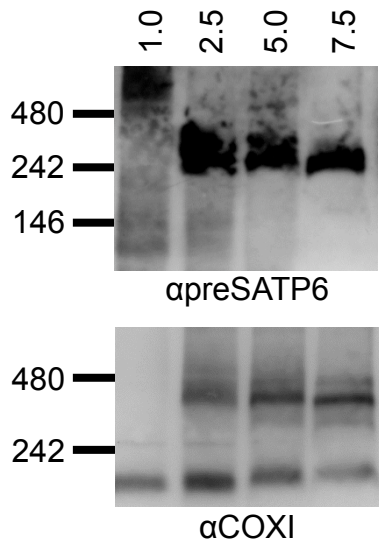

Fig. S4. Immunoblot analysis of immature anthers collected from TK-81mm-CMS. Total cellular proteins were lysed in the presence of digitonin at a digitonin/protein (w/w) ratio of 1.0, 2.5, 5.0, and 7.5. Gel blots were probed with αpreSATP6 or αCOXI. Size markers are shown on the left (kDa). The 250 kDa complex detected with apreSATP6 is stable in the digitonin/protein ratio range of 2.5 to 7.5. Note that the digitonin/protein ratio employed for Figs. 2, 4, 6, 7, S3, S6 and S7 was 5.0.

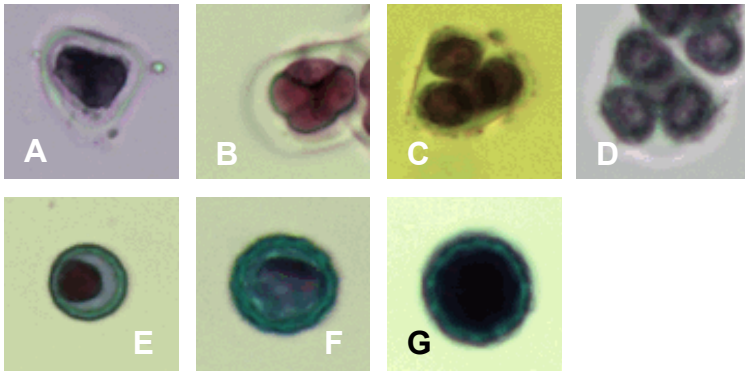

Fig. S5. Light microscopic images of anther contents stained with Alexander's dye (Alexander, 1969). Anthers were collected from NK-198. Collected anthers were immediately squashed in a droplet of Alexander's dye to stain their contents. The preparations were not incubated prior to observation. **A**, meiosis stage in which the microspore mother cell undergoes meiosis (depicted as M in Fig. 5); **B**, early tetrad stage in which meiosis is completed and four microspores firmly adhere to each other (Ta); **C**, middle tetrad stage in which the four microspores begin to separate (Tb); **D**, late tetrad stage in which the four microspores are clearly distinguished and the callose wall becomes thinner (Tc); **E**, early microspore stage in which the callose wall disappears, thereby releasing the microspores and a dense-stained globular structure is apparent inside of the microspore (Sa); **F**, late microspore stage in which the outer surface pattern becomes visible but the interior of the microspore is less stained than at the mature stage (Sb); **G**, mature stage in which the pollen grain is round, its surface exhibits a clear pattern, and interior of the pollen grain is deeply stained (P).

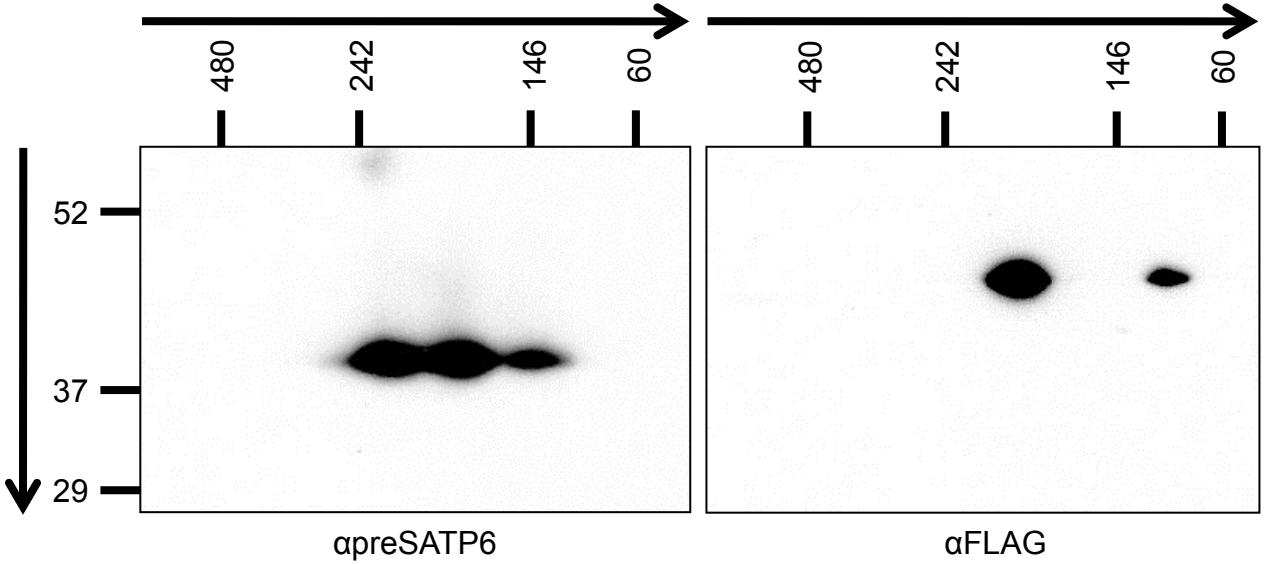

Fig. S6. Immunoblot analysis of mitochondrial proteins from NK-219mm-CMS callus expressing *bvORF20::flag*. Total mitochondrial proteins were lysed in the presence of digitonin, and then subjected to 2D-PAGE consisting of BN-PAGE (3-12%) for the first dimension (from left to right) and SDS-PAGE (4-12%) (from top to bottom). Gel blots were probed with αpreSATP6 or αFLAG. Size markers are shown in the top and left (kDa).

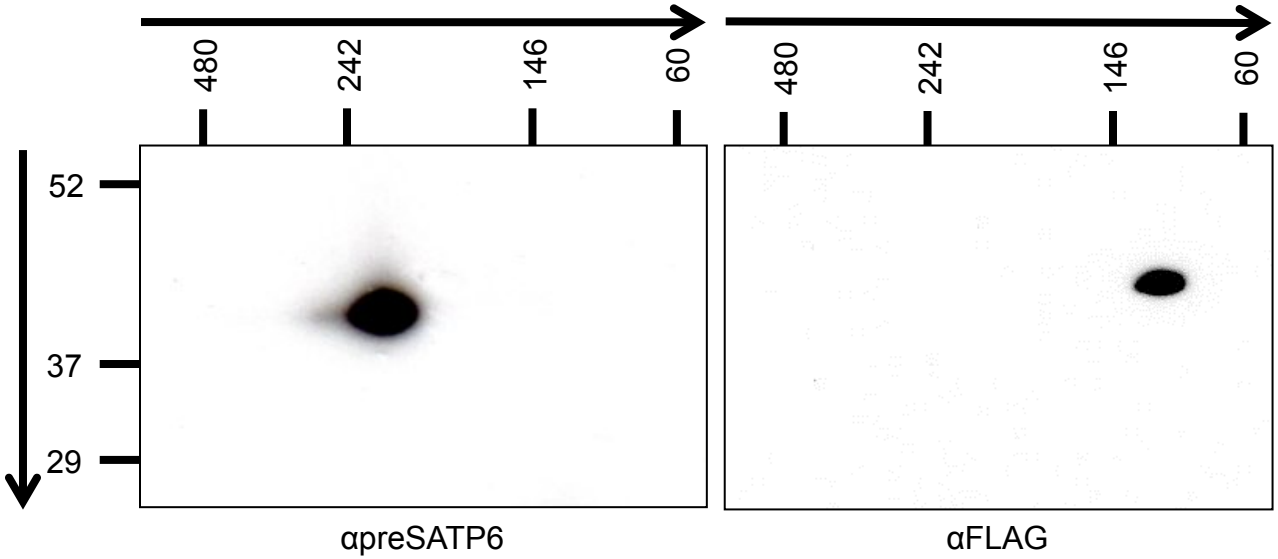

Fig. S7. Immunoblot analysis of mitochondrial proteins from NK-219mm-CMS callus expressing *bvORF20L::flag*. Total mitochondrial proteins were lysed in the presence of digitonin, and then subjected to 2D-PAGE consisting of BN-PAGE (3-12%) for the first dimension (from left to right) and SDS-PAGE (4-12%) (from top to bottom). Gel blots were probed with αpreSATP6 or αFLAG. Size markers are shown in the top and left (kDa).

Table S1. Nucleotide sequences of primers.

Names of primers	Nucleotide sequences
Primer 1	5'-AAAAGCTTTCCAATCCCACAAAAATCTG-3'
Primer 2	5'-ATTGGGCGCGCCCCATGGTAATTCTAAA-3'
Primer 3	5'-GGGGACAAGTTTGTACAAAAAAGCAGGCTAGGAATATCATAACCATT-3'
Primer 4	5'-GGGGACCACTTTGTACAAGAAAGCTGGGTGGTCCTGGATTGAGGGTT-3'
Primer 5	5'-TCAGGATTATAAGGATGATGATGATAAGTGACCATTTACCAACCAGCATCTTCTTTTAGCAGCTT-3'
Primer 6	5'-GTCACTTATCATCATCATCCTTATAATCCTGAAGACCTTGAATTGCACGTCCTGCTACAA-3'
Primer 7	5'-GGGGACAAGTTTGTACAAAAAAGCAGGCTCAGGAATATCATAGCCATT-3'
Primer 8	5'- GGGGACCACTTTGTACAAGAAAGCTGGGTTGCATGGGGTAATCACATCCA-3'
Primer 13	5'-AAAAAGCAGGCTCCGAGGAGACAGTTGATG-3'
Primer 14	5'-AGAAAGCTGGGTACTCATGTCGAGCCACAG-3'
Primer 15	5'-GGGGACAAGTTTGTACAAAAAAGCAGGCT-3'
Primer 16	5'-GGGACCACTTTGTACAAGAAAGCTGGGT-3'